Investigation of multi-layered graphene/silicon Schottky junction in oxidizing atmosphere

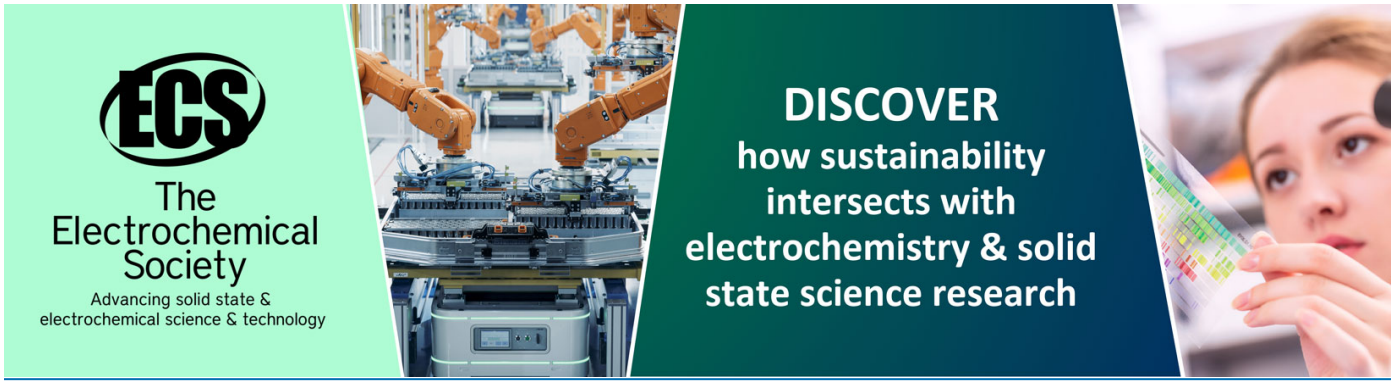

OPEN ACCESS
IOP Publishing
Journal of Physics D: Applied Physics
J. Phys. D: Appl. Phys. **54** (2021) 375104 (8pp)
https://doi.org/10.1088/1361-6463/ac0d71

Investigation of multi-layered graphene/silicon Schottky junction in oxidizing atmosphere

Filiberto Ricciardella[1,*], Maria Arcangela Nigro[2], Riccardo Miscioscia[3], Maria Lucia Miglietta[3] and Tiziana Polichetti[3]

[1] Department of Microelectronics, Delft University of Technology, Mekelweg 4, 2628 CD Delft, The Netherlands
[2] Indipendent Researcher, Cittanova, Italy
[3] National Agency for New Technologies Energy and Economic Sustainable Development (ENEA), Piazzale E. Fermi 1, Portici (Naples) I-80055, Italy

E-mail: filiberto.ricciardella@gmail.com

Received 17 March 2021, revised 28 May 2021
Accepted for publication 22 June 2021
Published 6 July 2021

Abstract

In this study, we investigate a Schottky junction based on solution-processed multilayered graphene (MLG). We present a rectifying device obtained with a straightforward approach, that is drop-casting a few microliters of MLG solution simultaneously onto Si, Si–SiO_2 and Si–SiO_2–Cr/Au surface. Monitoring the modulation of Schottky barrier height while operating in reverse bias, we study the behavior of such prepared MLG-Si/junction (MLG-Si/J) when exposed to oxidizing atmosphere, especially to nitrogen oxide (NO_2). We finally compare the sensing behavior of MLG-Si/J at 1 ppm of NO_2 with that of a chemiresistor-based on similarly prepared solution-processed MLG. Our study thus opens the path towards low-cost highly sensitive graphene-based heterojunctions advantageously fabricated without any complexity in the technological process.

Supplementary material for this article is available online

Keywords: graphene, Schottky junction, Schottky barrier height, gas-sensors, NO_2, liquid phase exfoliation

(Some figures may appear in colour only in the online journal)

1. Introduction

In the past decade, graphene has been proposed to form Schottky junction with a large variety of semiconductors such as Si, GaAs [1, 2], SiC [1, 3–5], GaN [6], CdS [7], CdSe [8]. Such hetero-junctions can be widely used in (opto)electronic applications, e.g. photodetectors [9–11], solar cells [12–14] and barristors [15]. In those applications, graphene can play the role of the metals because of the high mobility in both suspended and unsuspended layers, up to 2.5×10^4 or 2.0×10^5 $cm^2\ V^{-1}{\cdot}s^{-1}$, respectively [16–18]. Also, the transparency up to 98% in the visible range [19] would enable to lower the absorption of the light radiation typically generated by the metals. To ensure better performance of the devices in some of the aforementioned applications, high stability of the operating environment is strongly required. However, it is well known that graphene and its derivative is extremely reactive to the surrounding atmosphere [20–26]. The interaction with the ever-present gaseous species in the environment determines

* Author to whom any correspondence should be addressed.

the shift of the Fermi level which results in the modulation of the Schottky barrier height (SBH) [15, 27]. While on one hand the SBH's modulation might influence the performance of some devices, on the other hand it does not necessarily represent a downside. Operating with the Schottky junction, the interaction with the surrounding gases can be such advantageous as a transduction mechanism in the sensing field that the Schottky junction between graphene and Si has been promisingly proposed for the detection of several analytes [28–34]. To realize the junction, graphene is usually produced by techniques such as chemical vapor deposition (CVD) [28, 30–34] or mechanical cleavage [29, 35]. In both cases, either the synthesis of the material needs complex equipment and fabrication processes, as for the CVD, or an extremely low throughput is obtained through the peel-off of the graphite by mechanical cleavage [36].

In the current study, we fabricate the junction using the material synthesized in a low-cost alternative way, i.e. liquid phase exfoliation (LPE) of natural graphite. Although the solution-processed materials can result in dispersions with a certain distribution of the flakes' thickness and size [37, 38], we aim at fabricating both material and device more straightforwardly and with much less technologically complexity compared to the others described previously. We already reported the proof-of-concept of a similar device in previous works where we showed the behavior of the Schottky junction based on LPE-multi-layered graphene (later referred as MLG/Si-J) while interacting with an electron-donor analyte, such as ammonia (NH_3) [39–41]. Up to now, besides those reports, LPE-based Schottky junction has been partly investigated by another group only, despite the method reported in that work is rather a combination of LPE and CVD [42]. Following-up our prior works, in this paper, we study the sensing properties of solution-processed MLG/Si-J when exposed to an electron-acceptor target gas, such as NO_2. We also compare the sensing behavior of the Schottky junction with that of a solution-processed MLG-based chemi-resistor (CR), proving that the transduction mechanism relied on the SBH modulation is definitively more efficient compared to the change of resistivity induced in the CR. Our results are therefore consistent with those reported by Singh *et al* [31], even though originally obtained with a solution-processed low-cost-based MLG/Si-J.

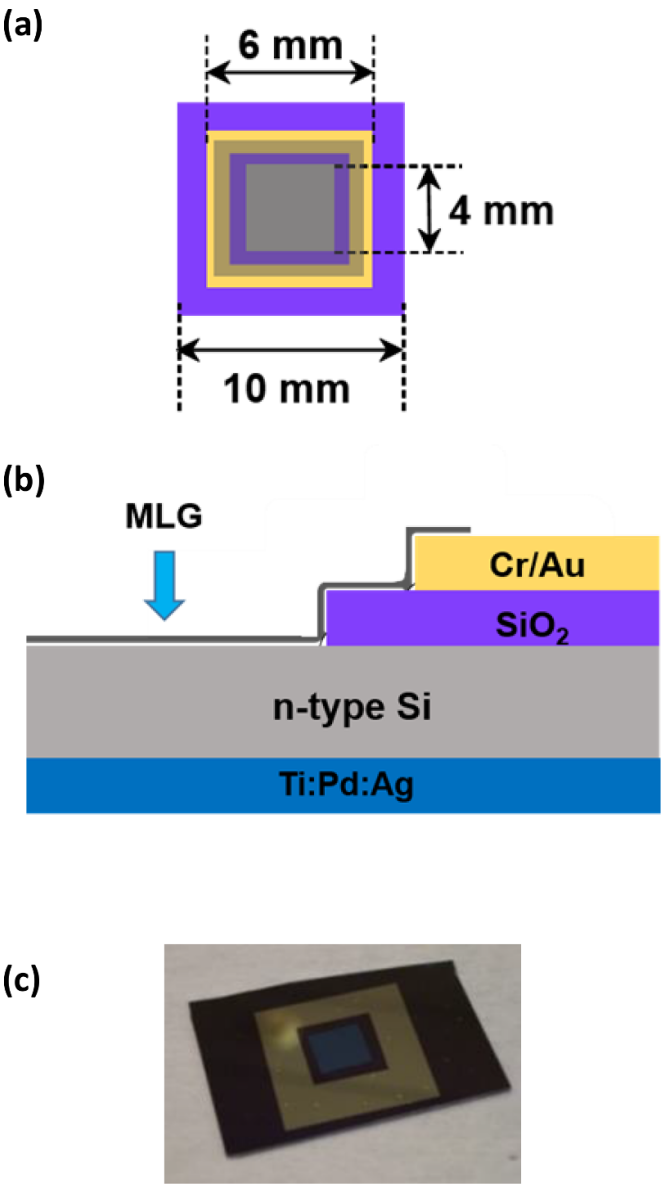

Figure 1. (a) Planar, (b) lateral view and (c) optical image of the fabricated device. The blue arrow in panel (b) indicates where MLG is in contact with Si to form the hetero-junction.

2. Materials and methods

We investigated MLG through a Renishaw inVia Reflex spectrometer equipped with an Ar laser ($\lambda = 514.5$ nm) and a 100× objective with a numerical aperture of 0.70. The surface topography was inspected through scanning electron microscope (SEM) Philips XL50, using a beam acceleration voltage of 15 kV.

To fabricate the Schottky junction, we adopted the structure depicted in figures 1(a) and (b) [43, 44]. As a substrate, we used an n-type heavily doped Si wafer ($\rho = 1$ Ωcm) covered with e-beam evaporated SiO_2 film (250 nm) excluding a square window of 16 mm^2. Around the Si window, onto the SiO_2 film we evaporated a Cr/Au (10 nm/100 nm) annulus, having the inner side 6 mm long. On the backside of the Si wafer, we deposited by e-beam an alloy of Ti/Pd/Ag serving as ohmic contact.

We synthesized MLG dispersing 2.5 mg of natural powdered graphite (Sigma-Aldrich, product 332461) in a mixture of 2-propanol and water used as a solvent to exfoliate the graphite [45]. After the exfoliation and purification steps detailed in previous reports [45, 46], we drop-casted few microliters of the MLG feed solution over the whole structure, simultaneously covering the Si window and the surrounding top electrical gold contact (figures 1(a) and (b)). MLG/Si-J is formed where MLG is in intimate contact with Si, as indicated by the blue arrow in figure 1(b). Figure 1(c) displays the optical image of the fabricated device.

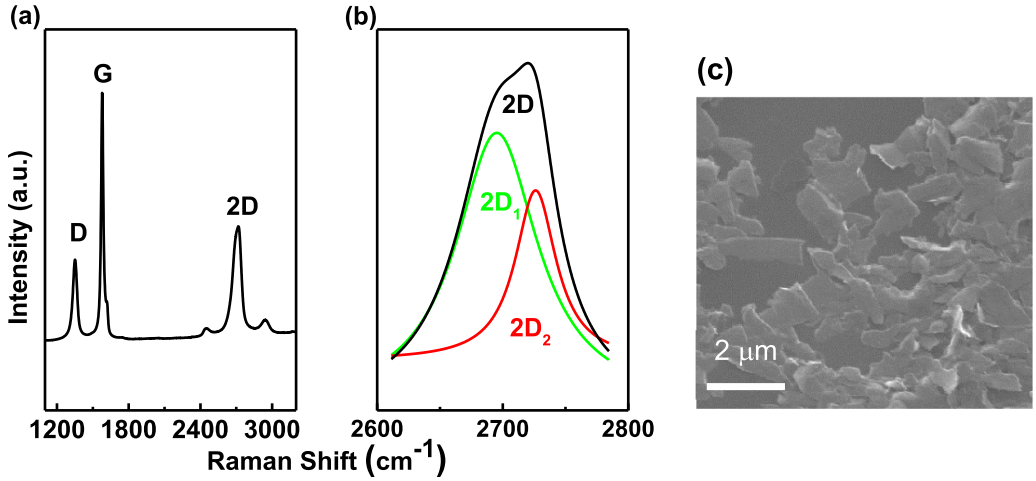

Figure 2. (a) Representative Raman spectrum of MLG, normalized to the intensity of the G band. (b) Magnification of the 2D band of panel (a) with the sub-components $2D_1$ (green line) and $2D_2$ (red line), located at ∼2695 cm^{-1} and ∼2726 cm^{-1}, respectively. (c) SEM image captured on MLG drop-casted on the substrate. Reproduced from [48]. © Royal Society of Chemistry. CC BY 3.0.

The electrical analysis was performed by a Keithley 4200 Semiconductor Characterization System connected to a Cascade Microtech Summit 11000 probe station, in ambient conditions at room temperature.

Afterwards, we exposed the device in a customized gas sensor characterization system comprising a stainless-steel chamber (0.4 dm^3) placed in a thermostatic box and provided with an electrical grounded connector for bias and conductance measurements. Temperature, pressure, relative humidity and flow rate of the analyte were kept constant at (22 ± 2) °C, (1.00 ± 0.05) bar, 50% and 500 sccm, respectively. Different concentrations of the analytes were obtained by a programmable mass flow controllers (MKS) and electro-pneumatic valves. During the measurements, we polarized the MLG/Si-J at a reverse constant DC voltage of −3 V with a Precision Power Supply TTi QL355 T. The current values were recorded by a high-resolution pico-ammeter (Keithley 6485).

3. Results and discussion

Figure 2 shows the results of the morphological characterizations performed on solution drop-casted onto the substrate. Figure 2(a) displays the representative Raman spectrum of the solution while figure 2(b) is the magnification of the 2D band, located at ∼2700 cm^{-1}. The profile, the features of the bands and the relative ratio of the deconvolved Lorentzian sub-components $2D_1$ (green line in figure 2(b)) and $2D_2$ (red line in figure 2(b)) indicate that the material forming the Schottky junction is mostly composed by MLG with a minimum thickness of 2–3 nm [39–41, 45–51]. The multilayered and jagged nature of the material is confirmed by the SEM image reported in figure 2(c) [48].

Figure 3 shows the *I*–*V* characteristic of the MLG/Si-J after drop-casting the MLG solution onto the bare device. For comparison, the *I*–*V* curve of the bare device is reported in the Supporting Information (figure S1 (available online at stacks.iop.org/JPD/54/375104/mmedia)). MLG/Si-J exhibits a Schottky diode behavior (figure 3(a)) with a rectification factor of about 100, as determined by the *I*–*V* characteristic in semi-logarithmic scale (inset figure 3(a)). The current I is expressed by the equation (1)) based on the thermionic emission model:

$$I = AA^*T^2 \exp\left(-\frac{q\varphi_B}{k_B T}\right)\left[\exp\left(\frac{qV}{\eta k_B T}\right) - 1\right] \qquad (1)$$

where A is the MLG/Si-J contact area, A^* the effective Richardson's constant for Si substrate, T the absolute temperature, φ_B the SBH, q the electron charge, k_B the Boltzmann constant, V the bias voltage and η the ideality factor of the diode [52].

For $V \gg \eta k_B T/q$, equation (1) can be rewritten as $I \approx I_S \exp\left(\frac{qV}{\eta k_B T}\right)$, where I_s is the saturation current [52], and rearranging the terms, the previous equation becomes:

$$\ln I = \ln I_S + \frac{qV}{\eta k_B T}. \qquad (2)$$

The linear fit of equation (2), in the range 75 ÷ 200 mV, enables to determine the ideality factor η and the saturation current I_s. The limits of the voltage range are determined by the value $3k_BT/q$ satisfying the conditions $V \gg \eta k_B T/q$ (with $\eta = 1$) and the voltage where the series resistance starts dominating, respectively [52].

From the slope of the fit (figure 3(b)), we extract $\eta \sim 2.25$, which is higher than the value of the ideal Schottky junction ($\eta = 1$). Values of η greater than 1 are usually attributed to the inhomogeneity at the interface with Si which determines deviations from the pure thermionic emission transport [1, 9, 34, 53–56]. Nevertheless, values comparable or much higher than the one reported herein have been largely reported in the literature, also in the case of graphene synthesized through different techniques, such as CVD [31, 32, 57, 58].

Manipulating the equation describing the saturation current $I \approx I_S \exp\left(\frac{qV}{\eta k_B T}\right)$, whose value is determined from the

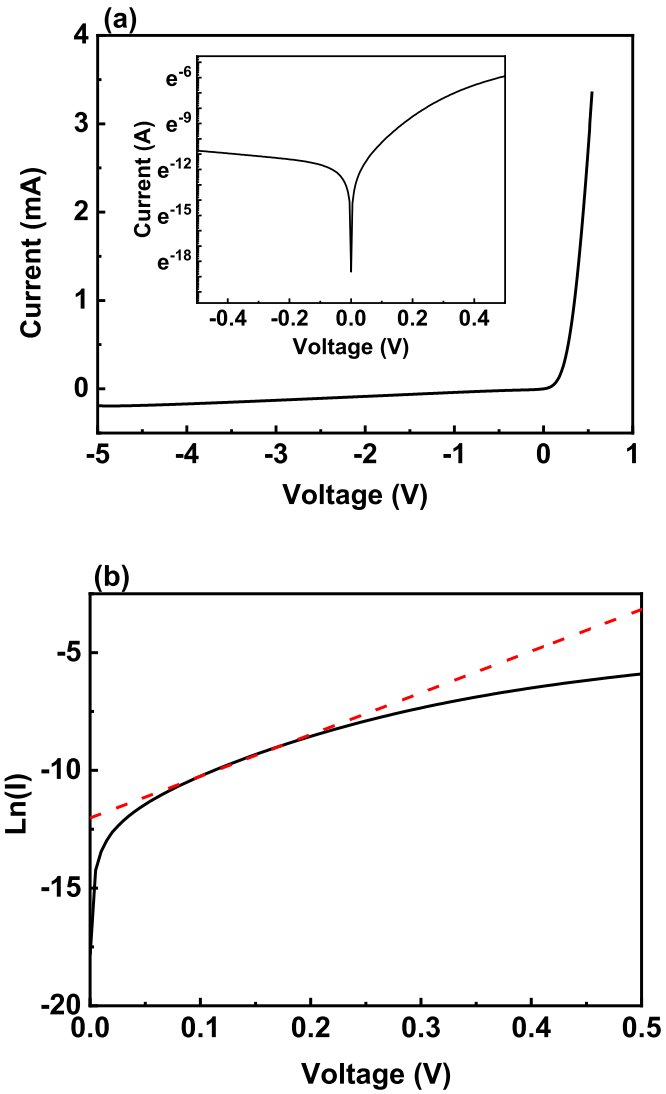

Figure 3. (a) I–V characteristic of the MLG/Si-J in linear and semi-logarithmic scale (inset). (b) Semi-logarithmic plot of the forward biased current with overlapped linear fit (red dashed line) to extract the factor of ideality η.

intercept of the straight line with the y-axis (figure 3(b)), we obtain φ_B from the equation (3):

$$\varphi_B = -\frac{k_B T}{q} \ln\left(\frac{I_S}{AA^* T^2}\right). \quad (3)$$

If we assume the entire uncovered Si window ($A = 0.16$ cm^2) as a MLG/Si-J contact area, $k_B T/q = 26$ mV at $T = 300$ K and $A^* = 112$ A cm^{-2} K^{-2} for n-Si substrate, we estimate the absolute value $\varphi_B \sim 0.68$ eV which is aligned with the values reported elsewhere [9, 14, 59]. Because of the drop-cast technique used to create the Schottky junction, it can happen that the contact area between the MLG feed solution and Si slightly differs from the nominal area of the Si window. The contact area parameter, however, does not dramatically affect the value of φ_B. We estimate that a large variation of A from 16 down to 9 mm^2, that is the area in case the Si window was 3 mm long in lateral side, would result in a decrease of $\varphi_B \sim 1\%$. Therefore, minimal variations of A induce negligible changes of SBH.

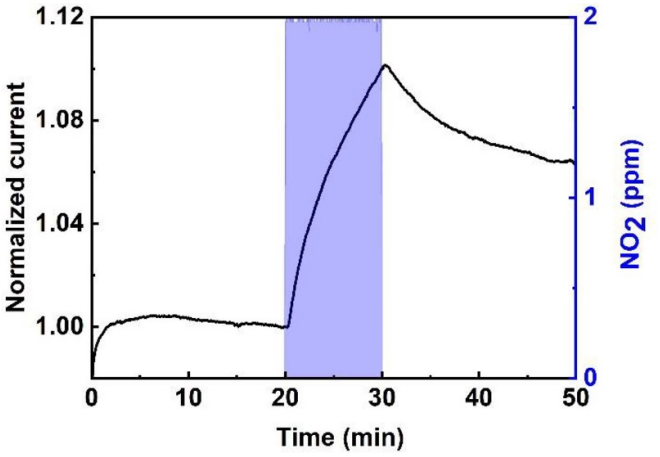

Figure 4. Real-time current behavior of MLG/Si-J upon exposure to 2 ppm of NO_2. The graph is normalized at the value of the current at the gas inlet. The pale blue rectangle highlights the exposure window.

The determination of φ_B permits to calculate the work function of MLG (later referred as W_G), according to the Schottky–Mott relation $W_G = \varphi_B + \chi_{Si}$, where $\chi_{Si} = 4.05$ eV is the electronic affinity of Si.

The estimated value in our case ($W_G \sim 4.73$ eV) is slightly higher than that usually reported for graphene, ranging between 4.3 and 4.6 eV, depending on the number of layers [60]. Provided that W_G also depends on the bias voltage [61], the small deviation of W_G might be ascribed to both the multi-layer nature and/or the p-doping of the material. Indeed, the MLG considered in this paper differs significantly from the material used in other works, e.g. graphene synthesized by CVD [62] or epitaxially grown on 6H-SiC [60, 63, 64]. Those techniques, although much more technologically complex and more expensive than LPE, usually guarantee a more accurate control of the number of layers. Yet, the inhomogeneity of the flakes' thickness usually associated to the solution-processed materials [37, 38] might influence some electrical parameters of the junction and the subsequent performance upon the analyte exposure.

Once the electrical properties were characterized, we investigated the sensing properties of MLG/Si-J in oxiding atmosphere using NO_2 as a target gas. We operated in reverse bias (-3 V) because of the exponential dependence of the saturation current from the SBH which is affected by the molecular absorption of NO_2, as reported in equation (1) [31].

Figure 4 shows the behavior of the saturation current when the device was exposed to 2 parts-per-million (ppm) of NO_2. When we injected the analyte into the test chamber (pale blue rectangle in figure 4), the signal keeps increasing for 10 min up to reach the maximum value I_{max} when the gas flow is interrupted. During the subsequent purge phase with N_2, the signal spontaneously and slowly tends to restore the initial state.

The real-time behavior is comparable with the results reported in previous works [46–50, 65–70], especially in terms of the kinetics of interaction between the sensing layers and the

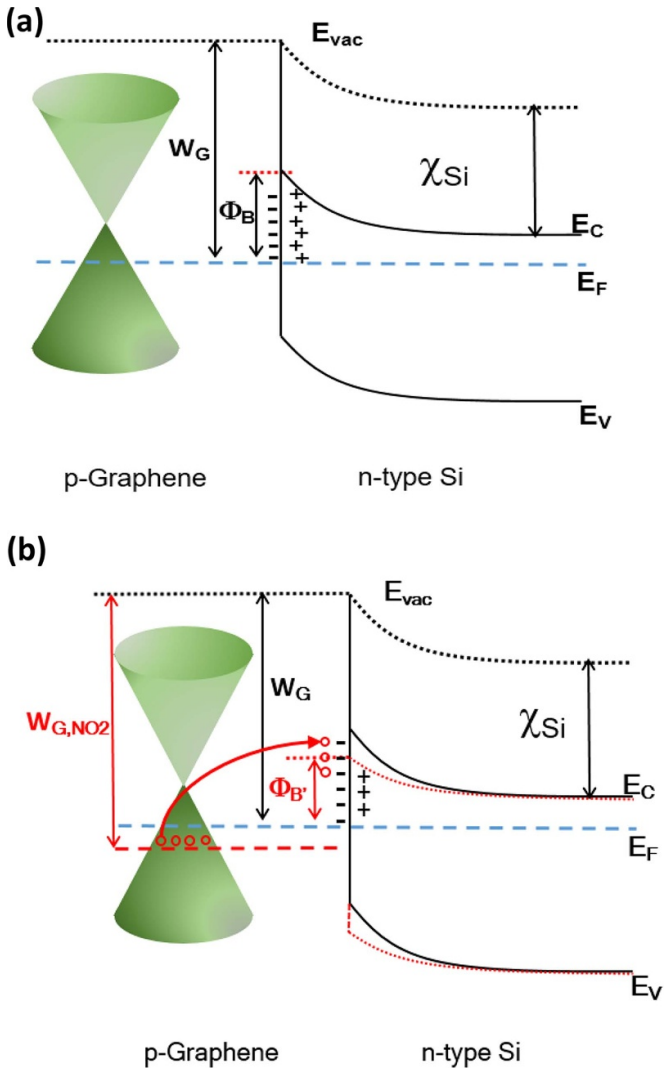

Figure 5. Band diagram of the heterojunction (a) before and (b) after the exposure to NO_2. For the sake of clarity, the band structure of graphene was designed similar as that of a single layer of graphene. E_{vac}, E_C, E_V and E_F indicate vacuum energy, conduction band, valence band and Fermi level of the n-type Si, respectively.

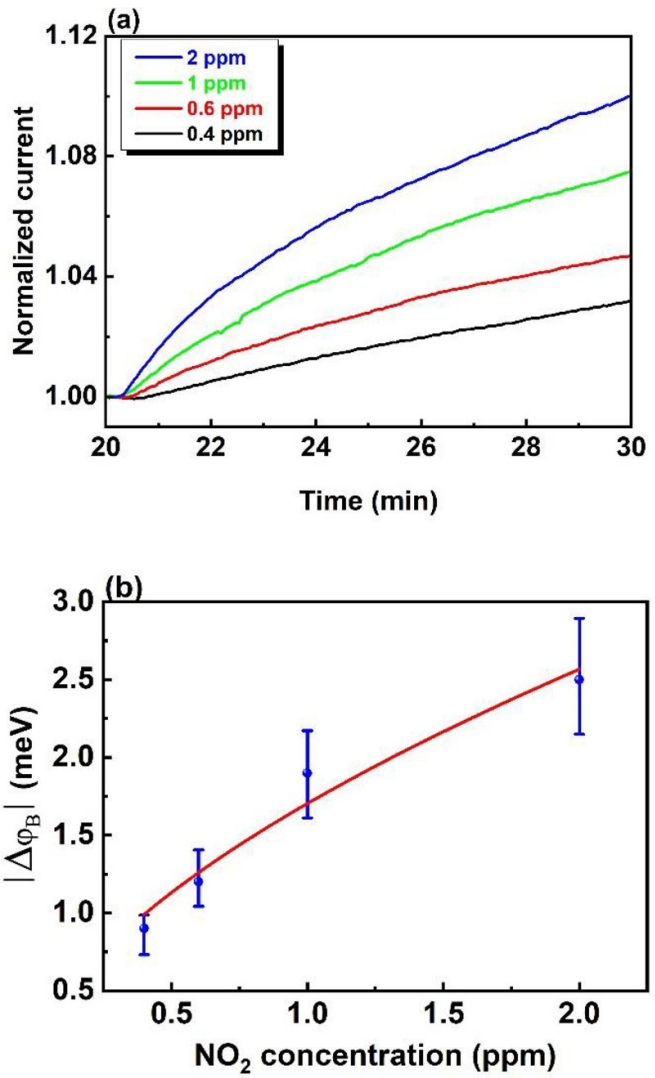

Figure 6. (a) Magnification of the signal recorded during the exposure at different concentrations of NO_2. The signals are normalized at the values I_0 prior to the gas inlet. (b) Absolute value of SBH vs NO_2 concentration as calculated from panel (a).

molecules during both exposure and purging phase. While in those works the authors reported on chemi-resistive devices, where the charge transfer induced a variation in the resistivity of the sensing layer, in the present paper, the behavior of the current is based on the SBH's modulation due to the interaction between the analyte and the MLG-Si/J [9]. The increase of I_S means a higher injection of the minority carriers (i.e. electrons) from p-doped MLG to the n-type Si. The I_S increase can be attributed solely to the lowering of SBH at the end of the adsorption process, as sketched in figure 5. In that figure, to easily visualize the physical mechanism and without lack of generalization, we draw up the bands of a single layer of graphene even though we are dealing with a mixture of multilayered material.

Compared to the pre-exposure (figure 5(a)), it can be seen that the holes donated by the NO_2 during the adsorption process recombine at the interface MLG-Si. Consequently, SBH ($\varphi_{B'}$) was lower (figure 5(b)) than the pre-exposed condition, as also reported by Singh *et al* [31], and the flow of electrons is favored from the p-type side of the junction, determining the increase of I_S.

Applying equation (3) to the graph in figure 4, we explicitly calculated the variation of the SBH induced by the exposure to 2 ppm of NO_2 as follows:

$$\Delta\varphi_B = -\frac{k_B T}{q}\ln\left(\frac{I_{max}}{I_0}\right) \quad (4)$$

where I_0 is the current immediately prior to the gas inlet (figure S2 (available online at stacks.iop.org/JPD/54/375104/mmedia)). The negative value of the SBH's variation ($\Delta\varphi_B \sim -2.5$ meV) further indicates that $\varphi_{B'} < \varphi_B$, i.e. SBH after the exposure is lower than SBH before the exposure. To strengthen more this conclusion, we exposed the MLG-Si/J to decreasing concentrations of NO_2 from 2 down to 0.4 ppm. Figure 6(a) shows the signal recorded during the

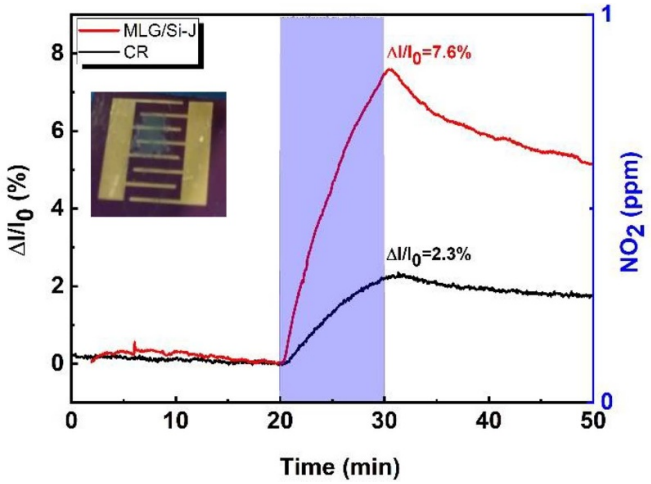

Figure 7. Percentage variation of the current vs time of MLG/Si-J (red line) and CR (black line) during the exposure to 1 ppm of NO_2 (pale blue rectangle). Inset: picture of the MLG-based CR [48]. Reproduced from [48]. © Royal Society of Chemistry. CC BY 3.0.

exposure window at different concentrations of NO_2. Introducing in equation (4) the values I_{max}/I_0 determined from figure 6(a), we accordingly obtained the variation of SBH. The absolute value of SBH plotted as a function of NO_2 concentration confirms our statement that the final SBH after each exposure is reduced compared to the pre-exposed situation (figure 6(b)).

The fit in figure 6(b) (red line) shows the dependence of SBH from the concentration C given by $\Delta\varphi_B \approx C^{\alpha}$, where we extrapolated $\alpha = 0.6 \pm 0.1$. Such a correlation, besides being in close agreement with our previous results obtained with other analytes [40], is well aligned with the outcomes reported in the literature, independently from the technique of graphene synthesis [15, 43, 71].

To finally illustrate the role of the SBH in the sensing mechanism of MLG-Si/J, we compared the behaviour of the junction with that of a CR. We thus referred to the device reported in our previous work [48], where MLG was synthesized via LPE using the same recipe as described in the present paper. The only difference between MLG-Si/J and CR is that, in case of CR, we fully covered the Si-bare substrate with a thin layer of SiO_2 before drop-casting MLG to insulate the metallic electrodes and sensing layer from Si. Despite the deposition of MLG on top of either Si or SiO_2, no differences in the wettability of MLG on both substrates were observed, fairly enabling the comparison of the two devices.

Figure 7 displays the representative dynamic behavior of CR and MLG-Si/J upon exposure to 1 ppm of NO_2. It can be observed a significant difference between the black and red curve during the exposure window, i.e. $(\Delta I/I_0)_{MLG\text{-}Si/J} \approx 3.3(\Delta I/I_0)_{CR}$. Because of the use of the similar solution-processed MLG in both cases, it is very likely that the difference can be ascribed to the mechanism of transduction taking place in either architectures. In MLG-Si/J operating in reverse bias, I_S exponentially depends on the SBH's modulation which is the parameter affected by the adsorption of the analyte's molecules. Conversely, in CR, the conductance variation is more linearly dependent from the analyte adsorption.

It is well known that the solution-processed materials might introduce a small degree of uncertainty in the features of both material and physical quantities of the devices. Nevertheless, although withdrawn with LPE-based MLG, our conclusions are not only independent from the techniques used to synthesize the sensing layer but also intrinsically due to the physics of the investigated devices. Furthermore, our achievements reveal particularly appealing as can be tailored without any complex fabrication process and tool.

4. Conclusions

We fabricated a Schottky device depositing few microliters of solution-processed MLG. The current–voltage investigation confirmed that we successfully realized a MLG-Si/J with a rectifying ratio roughly equal to 100 and an ideality factor $\eta = 2.25$. Such prepared hetero-junction was sensitive to NO_2 even at concentrations as low as 400 ppb. Analyzing the saturation current of the MLG-Si/J, we investigated the transduction mechanism relied on the SBH's modulation induced by the absorbed molecules. We finally compared the sensing behavior of MLG-Si/J with that of a CR-based on similarly prepared solution-processed MLG. We experimentally showed that, during the exposure at 1 ppm of NO_2, MLG-Si/J exhibited a signal that is roughly three times higher than the CR one. Our outcomes thus pave the route to efficiently fabricate low-cost sensitive gas sensors without any complexity in the technological process.

Data availability statement

All data that support the findings of this study are included within the article (and any supplementary files).

Acknowledgments

The authors are grateful to E. Massera (ENEA Portici, Italy) for the assistance in the use of the sensing set-up.

Author contributions

F R fabricated the devices, performed the sensing measurements, analysed the data, wrote the original draft, reviewed and edited the manuscript. M A N assisted with the electrical measurements. R M performed the electrical measurements. M A N and R M assisted in the interpretation of the electrical measurements. M L M synthesized the sensing material. T P conceived the idea of the experiment, assisted with the fabrication of the devices, the interpretation of the sensing measurements, the outline of the manuscript and supervised the final draft. All authors have read and agreed to the published version of the manuscript.

ORCID iDs

Filiberto Ricciardella https://orcid.org/0000-0002-9669-5649
Riccardo Miscioscia https://orcid.org/0000-0001-6586-4182

References

[1] Tongay S, Schumann T and Hebard A F 2009 Graphite based Schottky diodes formed on Si, GaAs, and 4H-SiC substrates *Appl. Phys. Lett.* **95** 222103
[2] Chen C C, Aykol M, Chang C C, Levi A F J and Cronin S B 2011 Graphene-Silicon Schottky Diodes *Nano Lett.* **11** 1863–7
[3] Reshanov S A, Emtsev K V, Speck F, Gao K, Seyller T K, Pensl G, Ley L, Physik A and Erlangen-nürnberg U 2008 Effect of an intermediate graphite layer on the electronic properties of metal/SiC contacts *Phys. Status Solidi Basic Res. Stat. Sol.* **245** 1369–77
[4] You A, Be M A Y and In I 2011 Schottky barrier between 6H-SiC and graphite: Implications for metal/SiC contact formation *Appl. Phys. Lett.* **242103** 10–13
[5] Sonde S, Giannazzo F, Raineri V, Yakimova R, Huntzinger J R, Tiberj A and Camassel J 2009 Electrical properties of the graphene/ 4H-SiC (0001) interface probed by scanning current spectroscopy *Phys. Rev.* B **80** 241406
[6] Tongay S, Lemaitre M, Schumann T, Berke K, Appleton B R, Gila B and Hebard A F 2011 Graphene/GaN Schottky diodes: Stability at elevated temperatures *Appl. Phys. Lett.* **99** 102102
[7] Ye Y *et al* 2010 High-performance single CdS nanowire (nanobelt) Schottky junction solar cells with Au/graphene Schottky electrodes *ACS Appl. Mater. Interfaces* **2** 3406–10
[8] Zhang L *et al* 2011 Graphene-CdSe nanobelt solar cells with Tunable configurations *Nano Res.* **4** 891–900
[9] Di Bartolomeo A 2016 Graphene Schottky diodes: an experimental review of the rectifying graphene/semiconductor heterojunction *Phys. Rep.* **606** 1–58
[10] Tao Z, Zhou D, Yin H, Cai B, Huo T, Ma J, Di Z, Hu N, Yang Z and Su Y 2020 Graphene/GaAs heterojunction for highly sensitive, self-powered Visible/NIR photodetectors *Mater. Sci. Semicond. Process.* **111** 104989
[11] Ezhilmaran B, Patra A, Benny S, Sreelakshmi M R, Akshay V V, Bhat S V and Rout C S 2021 Recent developments in the photodetector applications of Schottky diodes based on 2D materials *J. Mater. Chem.* C **9** 6122–50
[12] Song L, Yu X and Yang D 2019 A review on graphene-silicon Schottky junction interface *J. Alloys Compd.* **806** 63–70
[13] Bhopal M F, Lee D W, Rehman A and Lee S H 2017 Past and future of graphene/silicon heterojunction solar cells: a review *J. Mater. Chem.* C **5** 10701–14
[14] Kong X, Zhang L, Liu B, Gao H, Zhang Y, Yan H and Song X 2019 Graphene/Si Schottky solar cells: a review of recent advances and prospects *RSC Adv.* **9** 863–77
[15] Yang H *et al* 2012 Graphene barristor, a triode device with a gate-controlled Schottky barrier *Science* **1140** 1140
[16] Novoselov K S, Geim A K, Morozov S V, Jiang D, Katsnelson M I, Grigorieva I V, Dubonos S V and Firsov A A 2005 Two-dimensional gas of massless Dirac fermions in graphene *Nature* **438** 197–200
[17] Bolotin K I, Sikes K J, Jiang Z, Klima M, Fudenberg G, Hone J, Kim P and Stormer H L 2008 Ultrahigh electron mobility in suspended graphene *Solid State Commun.* **146** 351–5
[18] Bolotin K I, Sikes K J, Hone J, Stormer H L and Kim P 2008 Temperature-dependent transport in suspended graphene *Phys. Revi. Lett.* **096802** 1–4
[19] Nair R R, Blake P, Grigorenko A N, Novoselov K S, Booth T J, Stauber T, Peres N M R and Geim A K 2008 Fine structure constant defines visual transparency of graphene *Science* **320** 2–3
[20] Yang S, Jiang C and Wei S 2018 Gas sensing in 2D materials *Appl. Phys. Rev* **021304**
[21] Tian W, Liu X and Yu W 2018 Research progress of gas sensor based on graphene and its derivatives: a review *Appl. Sci.* **8** 1118
[22] Nag A, Mitra A and Chandra S 2018 Graphene and its sensor-based applications: a review *Sens. Actuators* A **270** 177–94
[23] Anichini C, Czepa W, Pakulski D, Aliprandi A, Ciesielski A and Samorì P 2018 Chemical sensing with 2D materials *Chem. Soc. Rev.* **47** 4860–908
[24] Yuan W and Shi G 2013 Graphene-based gas sensors *J. Mater. Chem.* A **1** 10078
[25] Zou C, Hu J, Su Y, Zhou Z, Cai B, Tao Z, Huo T, Hu N and Zhang Y 2020 Highly repeatable and sensitive three-dimensional γ-Fe2O3@reduced graphene oxide gas sensors by magnetic-field assisted assembly process *Sens. Actuators* B **306** 127546
[26] Rodner M, Bahonjic J, Mathisen M, Gunnarsson R, Ekeroth S, Helmersson U, Ivanov I G, Yakimova R and Eriksson J 2018 Performance tuning of gas sensors based on epitaxial graphene on silicon carbide *Mater. Des.* **153** 153–8
[27] Kim H, Lee K, Mcevoy N, Yim C and Duesberg G S 2013 Chemically modulated graphene diodes *Nano Lett.* **13** 2182–8
[28] Kim H, Lee K, Mcevoy N, Yim C and Duesberg G S 2013 Chemically modulated graphene diodes *Nano Lett.* **13** 2182–8
[29] Fattah A, Khatami S and Mayorga-martinez C C 2014 Graphene/silicon heterojunction schottky diode for vapors sensing using impedance spectroscopy *Small* **10** 4193–9
[30] Uddin A, Singh A K and Sudarshan T S 2014 Functionalized graphene/silicon chemi-diode H 2 sensor with tunable sensitivity *Nanotechnology* **25** 125501
[31] Singh A, Sudarshan T and Koley G 2013 Tunable reverse-biased graphene/silicon heterojunction schottky diode sensor *Small* **10** 1555–65
[32] Sinha D and Lee J U 2014 Ideal graphene/silicon Schottky junction diodes *Nano Lett.* **14** 4660–4
[33] Rajput S, Chen M X, Liu Y, Li Y Y, Weinert M and Li L 2013 Spatial fluctuations in barrier height at the graphene–silicon carbide Schottky junction *Nat. Commun.* **4** 1–7
[34] Yim C, Mcevoy N, Duesberg G S, Yim C, Mcevoy N and Duesberg G S 2013 Characterization of graphene-silicon Schottky barrier diodes using impedance spectroscopy *Appl. Phys. Lett.* **103** 193106
[35] Tongay S, Schumann T, Miao X, Appleton B R and Hebard A F 2011 Tuning Schottky diodes at the many-layer-graphene/semiconductor interface by doping *Carbon N.* Y **49** 2033–8
[36] Novoselov K S, Fal V I, Colombo L, Gellert P R, Schwab M G and Kim K 2012 A roadmap for graphene *Nature* **490** 192–200
[37] Coleman J N 2013 Liquid exfoliation of defect-free graphene *Acc. Chem. Res.* **46** 14–22
[38] Backes C *et al* 2020 Production and processing of graphene and related materials *2D Mater.* **7** 022001
[39] Nigro M A, Faggio G, Fedi F, Polichetti T, Miglietta M L, Massera E, Di Francia G and Ricciardella F 2015 Cross interference effects between water and NH3 on a sensor based on graphene/silicon Schottky diode *Proc. 2015 18th*

AISEM Annu. Conf. AISEM 2015 (https://doi.org/10.3205/oc000028)
[40] Polichetti T *et al* 2014 Graphene-based Schottky device detecting NH3 at ppm level in environmental conditions *Proc. Eng.* **87** 232–5
[41] Polichetti T *et al* 2014 Graphene-Si Schottky diode in environmental conditions at low NH3 ppm level *2014 IEEE 9th Nanotechnology Materials and Devices Conf., NMDC 2014* (https://doi.org/10.1109/NMDC.2014.6997412)
[42] Mohammed M, Li Z, Cui J and Chen T 2012 Junction investigation of graphene/silicon Schottky diodes *Nanoscale Res. Lett.* **7** 1
[43] Tongay S, Lemaitre M, Miao X, Gila B, Appleton B R and Hebard A F 2012 Rectification at graphene-semiconductor interfaces: zero-gap semiconductor-based diodes *Phys. Rev.* X **2** 1–10
[44] Capasso A *et al* 2014 Cyclododecane as support material for clean and facile transfer of large-area few-layer graphene *Appl. Phys. Lett.* **105** 113101
[45] Fedi F, Miglietta M L, Polichetti T, Ricciardella F, Massera E, Ninno D and Di Francia G 2015 A study on the physicochemical properties of hydroalcoholic solutions to improve the direct exfoliation of natural graphite down to few-layers graphene *Mater. Res. Express* **2** 035601
[46] Ricciardella F, Massera E, Polichetti T, Miglietta M L and Di Francia G 2014 A calibrated graphene-based chemi-sensor for sub parts-per-million NO 2 detection operating at room temperature *Appl. Phys. Lett.* **104** 1–6
[47] Miglietta M L, Massera E, Romano S, Polichetti T, Nasti I, Ricciardella F, Fattoruso G and Di Francia G 2011 Chemically exfoliated graphene detects NO_2 at the ppb level *Proc. Eng.* **25** 1145–8
[48] Ricciardella F, Vollebregt S, Polichetti T, Miscuglio M, Alfano B, Miglietta M L, Massera E, Di Francia G and Sarro P M 2017 Effects of graphene defects on gas sensing properties towards NO2 detection *Nanoscale* **9** 6085–93
[49] Ricciardella F, Alfano B, Loffredo F, Villani F, Polichetti T, Miglietta M L, Massera E and Di Francia G 2015 Inkjet printed graphene-based chemi-resistors for gas detection in environmental conditions *Proc. 2015 18th AISEM Annual Conf., AISEM 2015*
[50] Alfano B, Polichetti T, Mauriello M, Miglietta M L, Ricciardella F, Massera E and Di Francia G 2016 Modulating the sensing properties of graphene through an eco-friendly metal-decoration process *Sens. Actuators* B **222** 1032–42
[51] Alfano B, Polichetti T, Massera E, Miglietta M L, Di Francia G, Ricciardella F and Mauriello M 2015 Tailoring the selectivity of chemical sensors based on graphene decorated with metal nanoparticles *2015 XVIII AISEM Annual Conf.*
[52] Sze S M 1981 *Physics of Semiconductor Devices* (New York: Wiley)
[53] Tung R T 2014 The physics and chemistry of the Schottky barrier height *Appl. Phys. Rev.* **1** 011304
[54] Tung R T 2001 Recent advances in Schottky barrier concepts *Mater. Sci. Eng. R* **35** 1–138
[55] Haick H, Ambrico M, Ligonzo T, Tung R T and Cahen D 2006 Controlling semiconductor/metal junction barriers by incomplete, nonideal molecular monolayers *J. Am. Chem. Soc.* **128** 6854–69
[56] Li Y, Long W and Tung R T 2012 Inhomogeneous ohmic contacts: barrier height and contact area determination *Appl. Phys. Lett.* **101**
[57] Cui T *et al* 2013 Enhanced efficiency of graphene/silicon heterojunction solar cells by molecular doping *J. Mater. Chem.* A **1** 5736–40
[58] Luongo G, Di Bartolomeo A and Giubileo F 2018 Electronic properties of graphene/p-silicon Schottky junction *J. Phys. D: Appl. Phys* **51** 255305
[59] Li X, Zhu H, Wang K, Cao A, Wei J, Li C, Jia Y, Li Z, Li X and Wu D 2010 Graphene-on-silicon schottky junction solar cells *Adv. Mater.* **22** 2743–8
[60] Hibino H, Kageshima H, Kotsugi M, Maeda F, Guo F Z and Watanabe Y 2009 Dependence of electronic properties of epitaxial few-layer graphene on the number of layers investigated by photoelectron emission microscopy *Phys. Rev.* B **79** 1–7
[61] Yu Y, Zhao Y, Ryu S, Brus L E, Kim K S and Kim P 2009 Tuning the graphene work function by electric field effect *Nano Lett.* **9** 340–4
[62] Yan R *et al* 2014 Determination of graphene work function and graphene-insulator-semiconductor band alignment by internal photoemission spectroscopy *Appl. Phys. Lett.* **101** 022105
[63] Filleter T, Emtsev K V, Seyller T and Bennewitz R 2008 Local work function measurements of epitaxial graphene *Appl. Phys. Lett.* **93** 133117
[64] Nomani M W K, Shields V, Tompa G, Sbrockey N, Spencer M G, Webb R A and Koley G 2012 Correlated conductivity and work function changes in epitaxial graphene *Appl. Phys. Lett.* **100** 092113
[65] Miglietta M, Polichetti T, Massera E, Nasti I, Ricciardella F, Romano S and Di Francia G 2012 *Sub-PPM nitrogen dioxide conductometric response at room temperature by graphene flakes based layer* vol 109 (LNEE)
[66] Ricciardella F, Vollebregt S, Polichetti T, Alfano B, Massera E and Sarro P M 2017 An innovative approach to overcome saturation and recovery issues of CVD graphene-based gas sensors *Proc. IEEE Sens.* 1224–6
[67] Ricciardella F, Polichetti T, Vollebregt S, Alfano B, Massera E and Sarro L 2019 Analysis of a calibration method for non-stationary CVD multi-layered graphene-based gas sensors *Nanotechnology* **30** 385501
[68] Ricciardella F, Lee K, Stelz T, Hartwig O, Prechtl M, Mccrystall M, Mcevoy N and Duesberg G S 2020 Calibration of nonstationary gas sensors based on two-dimensional materials *ACS Omega* **5** 5959–63
[69] Fedi F, Ricciardella F, Miglietta M L, Polichett T, Massera E and Di Francia G 2015 Easy recovery method for graphene-based chemi-resistors *Second National Conf. on Sensors* (*Rome*, *19–21 February 2014*) vol 319 ed D Compagnone, F Baldini, C Di Natale, G Betta and P Siciliano pp 203–6
[70] Ricciardella F, Vollebregt S, Polichetti T, Alfano B, Massera E and Sarro P M 2016 High sensitive gas sensors realized by a transfer-free process of CVD graphene *IEEE Sensors* (*Orlando*, *30 October - 3 November*) pp 697–9
[71] An Y, Behnam A, Pop E and Ural A 2013 Metal-semiconductor-metal photodetectors based on graphene/p -type silicon Schottky junctions *Appl. Phys. Lett.* **102** 013110